PHYSICAL REVIEW D VOLUME 40, NUMBER 3 1 AUGUST 1989

Exclusive semileptonic decays of B and D mesons

James M. Cline and William F. Palmer
Department of Physics, The Ohio State University, Columbus, Ohio 43210

G. Kramer
II. Institut für Theoretische Physik der Universität Hamburg, D-2000 Hamburg 50, West Germany
(Received 20 March 1989)

Exclusive semileptonic decays of D and B mesons to one and two pseudoscalar mesons are studied with respect to form-factor dependence, finite-width effects in intermediate resonant states, and nonresonant background terms calculated from chiral Lagrangians. Branching ratios, electron decay spectra, and asymmetry parameters for angular distributions are given for Cabibbo-Kobayashi-Maskawa-favored and -unfavored transitions, and compared to experimental data.

I. INTRODUCTION

The study of semileptonic decays of bottom mesons is of particular interest for determining the Cabibbo-Kobayashi-Maskawa (CKM) mixing parameters V_{cb} and V_{ub}. To extract these parameters from the measured lepton spectrum or other observables of B-meson decays one needs theoretical input in the form of weak-current matrix elements between the initial B meson and the possible final hadron states. Weak decays of D and B mesons are clearly nonperturbative processes and cannot be calculated reliably from the QCD Lagrangian. Therefore one relies on phenomenological models. Originally the free-quark-decay model[1] (with and without QCD corrections[2]) was the favored tool for discussing the semileptonic decays of heavy quarks. It is thought to give a reasonable description of the absolute decay rates and perhaps also of the semileptonic branching ratios. But, as has been emphasized many times, and in much detail recently by Isgur *et al.*,[3] it is not able to predict the shape of the lepton spectrum, in particular the shape and normalization of the $B \to X e \bar{\nu}_e$ end-point region, which is the interesting region for determining V_{ub}. This is the region of low recoil masses m_X, which is controlled by a set of discrete states: D, D^*, etc., in the case of B decays via $b \to c$ transitions or π, ρ, η, η', etc., for $b \to u$ transitions and similarly in the case of semileptonic D decays. Thus the study of exclusive semileptonic decays, of which the lepton spectrum is built, is a more realistic endeavor than the free-quark-decay approach, if the spectra are to be understood, especially in the end-point region.

In general we limit the discussion to the most simple and low-lying states and do not aim at the description of the complete lepton spectrum. In some cases, however, it seems that these low-lying states almost exhaust the semileptonic decay rate. $D \to K, K^*$ is such a case, so that a realistic description of the whole lepton spectrum is possible.

In order to get better insight into the validity of the phenomenological models, it is advisable to test them in cases where the weak mixing angles are known, for example, D decays with $c \to s$ transitions and B decays with $b \to c$. With the understanding obtained from these cases one might try to model the $b \to u$ transitions in B decay like $B \to \pi$, $\pi\pi$, $\pi\rho$, η, η', etc., which provides information on V_{ub}. Therefore we shall consider all semileptonic transitions of D and B mesons to one and to two pseudoscalar mesons on the same footing.

This field is presently under much experimental[4] and theoretical investigation. On the experimental side the semileptonic decay modes $D \to K$ (Refs. 4 ad 5), $D \to K^*$ (Ref. 4), and $B \to D^*$ (Refs. 4 and 6) have been clearly identified. The theoretical side of the field is much older. Rough estimates for exclusive decay rates were given already in (Ref. 1). Later work employed current algebra,[7] flavor-SU(4) symmetry, and various quark-model approaches to calculate individual form factors in transitions to final pseudoscalar, vector, or higher spin states.[8] In Ref. 9 effective chiral Lagrangians including a Wess-Zumino term have been used to predict weak matrix elements, especially for final states with two pseudoscalars. The chiral Lagrangian yields constraints on the weak matrix elements at very low energies, which are fully determined by the pion decay constant. This approach is particularly suited to calculate K_{e4} decays, which occur almost at threshold, and less suitable for the semileptonic decays of the heavier mesons, such as D and B, which are characterized by a large energy release. In the latter case the low-energy chiral approximation had to be improved by pole enhancements describing final-state interactions in intermediate states. These pole enhancement factors, however, were quite *ad hoc* and left no room to introduce sufficient structure into the weak transition matrix elements to vector-resonance intermediate states.

It is one of the purposes of this paper to remedy this drawback. We shall write down weak transition amplitudes to two pseudoscalars which have the same structure concerning transitions to intermediate vector-meson states as some of the models in Ref. 8 and have in addition the constraints arising from low-energy theorems codified in the chiral Lagrangian.[9] The low-energy constraints lead to additional terms, which we consider as a

reasonable model for a nonresonant background underneath the dominant resonant contribution. Unfortunately these contributions cannot be taken too seriously as they come from the lowest-order tree diagrams in an effective chiral Lagrangian. Because the D and B mesons are heavier than the chiral-symmetry-breaking scale $\Lambda_{\rm CSB}\sim 1$ GeV, there would be significant (and incalculable) contributions from higher-derivative interactions, loop diagrams, and higher-order symmetry-breaking terms. Therefore the current-algebra terms must be regarded as an educated guess rather than a quantitative estimate of the nonresonant contributions. It would certainly be wrong to omit them, even though their exact form is not predicted. Of course, such nonresonant terms will be relatively more important the larger the width of the intermediate resonance state is. Therefore they are more relevant for $D\to\rho$ than for $D\to K^*$ transitions. We expect them to be negligible for $B\to D^*$, but important for $B\to\rho$ transitions. This approach for semileptonic transitions of B's and D's to two pseudoscalar final states is in the same spirit as an extension of the chiral-Lagrangian framework to mainly electromagnetic transitions by two of us.[10] In this work we constructed transition amplitudes for $\eta,\eta'\to\pi^+\pi^-\gamma$, K_{e4}, $\omega\to\pi^+\pi^-\pi^0$, and $\gamma\to\pi^+\pi^-\pi^0$ that respect the low-energy theorems but also have realistic vector-meson pole continuation in the intermediate state.

In Sec. II we present the weak vector- and axial-vector-current matrix elements for $D\to K$ and $D\to K\pi$ with realistic intermediate pole structure in the case of $D\to K\pi$. From this the structure functions of the hadron tensor are derived, which determine the partial semileptonic width, the lepton spectrum, and the differential distribution of the lepton-neutrino invariant mass. Section III is reserved for the numerical results. We give results for D,B going to one pseudoscalar, just for completeness, and D,B going to two pseudoscalar mesons. For the latter case we consider contact terms based on the chiral Lagrangian representing nonresonant background and compare with the cases of no contact term and with the zero-width approximation. We discuss how the results depend on form factors and try to determine these form factors by comparing the helicity structure with recently measured parameters of the decay angular distribution of the vector-meson decay products. Section IV contains a summary and the conclusions.

II. SEMILEPTONIC DECAY SPECTRUM AND PARTIAL WIDTH

Following Wilson[8] and Chao *et al.*,[9] we write the total semileptonic decay rate as

$$\Gamma=\frac{2G_F^2 f(\theta_C)}{m_1(2\pi)^2}\int\frac{d^3k}{2k_0}\frac{d^3k'}{2k_0'}H^{\mu\nu}l_{\mu\nu} \tag{1}$$

with the lepton tensor

$$l_{\mu\nu}=k_\mu k'_\nu+k'_\mu k_\nu-k'\cdot k\,g_{\mu\nu}+i\epsilon_{\mu\nu\alpha\beta}k^\alpha k'^\beta \tag{2}$$

and the hadron tensor

$$H_{\mu\nu}=\sum_X\prod_{i=2}^n\int\frac{d^3p_i}{2p_{i0}(2\pi)^{3(n-1)}}\delta^{(4)}\left[p_1-q-\sum_{i=2}^n p_i\right]\times\langle D(p_1)|J_\mu^\dagger(q)|X(p_2,p_3,\ldots)\rangle\times\langle X(p_2,p_3,\ldots)|J_\nu(q)|D(p_1)\rangle\ . \tag{3}$$

The momenta correspond to a general process

$$p_1\to p_2+p_3+\cdots+k+k'\ , \tag{4}$$

where p_i are momenta of hadron decay products, k is the electron momentum, k' the neutrino momentum, $q=k+k'$ the momentum transfer to the lepton system, and m_1 the decaying meson mass. We shall integrate over the final hadronic momenta for single-pseudoscalar and two-pseudoscalar particle states, and vector-meson states. $H_{\mu\nu}$ is a dimensionless function of p_1, the momentum of the decaying meson, and q. We have neglected the lepton mass.

Instead of the variables k and k', describing the lepton system, we introduce new variables

$$x=\frac{2k_0}{m_1},\quad t=\frac{q^2}{m_1^2},\quad \mu^2=\frac{(p_1-q)^2}{m_1^2}\ , \tag{5}$$

where k_0 is the energy in the rest frame of particle 1. The width Γ is then given by

$$\Gamma=\frac{G_F^2 f(\theta_C)m_1^3}{8}\int dx\int dt\int d\mu^2 H^{\mu\nu}l_{\mu\nu} \tag{6}$$

with the integration boundaries

$$\mu_{\rm min}^2\le\mu^2\le 1-x,\quad 0\le t\le x(1-\mu^2-x)/(1-x)\ , \tag{7}$$

where $\mu_{\rm min}^2 m_1^2$ is the smallest mass appearing in the intermediate state.

The hadron tensor, in its most general form, has the decomposition

$$\begin{aligned}H_{\mu\nu}m_1^2=&-g_{\mu\nu}H_1m_1^2+p_{1\mu}p_{1\nu}H_2\\&+i\epsilon_{\mu\nu\alpha\beta}p_1^\alpha q^\beta H_3+q_\mu q_\nu H_4\\&+(p_{1\mu}q_\nu+q_\mu p_{1\nu})H_5+i(p_{1\mu}q_\nu-q_\mu p_{1\nu})H_6\ ,\end{aligned} \tag{8}$$

where the H_i are real functions of μ^2 and t. Only the first three structure functions contribute when we neglect the lepton mass, $q^\mu l_{\mu\nu}=l_{\mu\nu}q^\nu=0$. Substituting this decomposition into the width formula, we obtain

$$\Gamma=\frac{G_F^2 f(\theta_C)m_1^5}{8}\int dx\,dt\,d\mu^2\{tH_1(\mu^2,t)+\tfrac{1}{2}[x(1-\mu^2-x)-t(1-x)]H_2(\mu^2,t)+\tfrac{1}{2}t(2x-1-t+\mu^2)H_3(\mu^2,t)\}\ , \tag{9}$$

where $f(\theta_C)$ stands for the appropriate weak-mixing matrix element.

Note the electron momentum dependence arises only from the factors of x in the integrand and in the integration boundaries. Suppressing the curly-bracketed integrand in Eq. (9) these limits are

$$\Gamma=\frac{G_F^2 f(\theta_C) m_1^3}{8}\int_{\mu^2_{\min}}^{\mu^2_{\max}} d\mu^2 \int_0^{(1-\mu)^2} dt \int_{x_-}^{x_+} dx\{\ \}$$

$$=\frac{G_F^2 f(\theta_C) m_1^3}{8}\int_{\mu^2_{\min}}^{\mu^2_{\max}} d\mu^2 \int_0^{1-\mu^2} dx \int_0^{x[1-\mu^2/(1-x)]} dt\{\ \}, \tag{10}$$

where

$$x_\pm=\tfrac{1}{2}(1-\mu^2+t)\pm\tfrac{1}{2}\sqrt{(1-\mu^2+t)^2-4t}\ . \tag{11}$$

The expression (8) yields the most general form of the lepton spectrum $d\Gamma/dx$. From the definition of $H_{\mu\nu}$ in Eq. (3) it is obvious that $r_\mu^* H^{\mu\nu} r_\nu \geq 0$ for any r_μ. This condition leads to the following positivity constraints (Wilson, Ref. 8):

$$\Delta^2 H_2 + t H_1 \equiv \Delta^2 H_0 \geq 0, \quad H_1 \pm \Delta H_3 \equiv \Delta^2 H_\pm \geq 0\ , \tag{12}$$

$$\Delta=\tfrac{1}{2}\sqrt{(1+\mu^2-t)^2-4\mu^2}=p/m_1\ , \tag{13}$$

where p is the momentum $2m_1 p=[\lambda(tm_1^2,\mu^2 m_1^2,m_1^2)]^{1/2}$ of the intermediate state $X(p_2,p_3,\ldots)$ in the D-meson rest system and where $\lambda(a,b,c)=a^2+b^2+c^2-2ab-2ac-2bc$. In terms of the positive functions H_+, H_-, and H_0 the total width can be written

$$\Gamma=\frac{G_F^2 f(\theta_C) m_1^5}{32}\times\int dx\,dt\,d\mu^2[tH_+(\mu^2,t)(x_+-x)^2 + tH_-(\mu^2,t)(x-x_-)^2 + 2H_0(\mu^2,t)(x_+-x)(x-x_-)]\ . \tag{14}$$

Instead of the variable x we can introduce into Eq. (14) the angle θ, which is the polar angle between the momentum of the intermediate state X and the lepton l^- in the $(l^-\bar{\nu}_l)$ c.m. system. The relation between x and $\cos\theta$ is

$$2m_1 p\cos\theta=m_1^2-m_X^2+q^2-4m_1 k_0\ , \tag{15}$$

or, if written in terms of μ^2, t, and x,

$$2\Delta\cos\theta=1-\mu^2+t-2x\ . \tag{16}$$

Then we get, for Γ,

$$\Gamma=\frac{G_F^2 f(\theta_C) m_1^5}{32}\times\int dx\,dt\,d\mu^2[t\Delta^2 H_+(\mu^2,t)(1+\cos\theta)^2 + t\Delta^2 H_-(\mu^2,t)(1-\cos\theta)^2 + 2\Delta^2 H_0(\mu^2,t)(1-\cos^2\theta)]\ . \tag{17}$$

From Eq. (17) it is clear that H_+, H_-, and H_0 must be the helicity projections of $H_{\mu\nu}$, where the helicity $\lambda=\pm,0$ is the helicity label of the current.[11] It is clear that each of the terms in Eq. (17) must separately be positive. The problem of finding the lepton spectrum or any other differential distribution is now reduced to finding the three structure functions H_1, H_2, H_3 or their equivalents H_+, H_-, H_0.

In the following we evaluate H_1, H_2, and H_3 for final hadronic states of one and two pseudoscalar mesons and vector-meson resonances. The VA interference term is contained in H_3 and does not contribute to the total decay rate but does influence the electron spectrum shape. The effect in D decay is to shift the spectrum to lower electron momentum and in B decay to higher electron momentum.

For the processes with one pseudoscalar in the final state, let us consider the example

$$D^+\to\bar{K}^0+e^++\nu$$

or

$$(D^0\to\pi^++e^-+\bar{\nu})=\sqrt{2}(D^+\to\pi^0+e^++\nu)\ .$$

With the notation $p_1\to p_2+k+k'$, the transverse part of the current is

$$J_\mu=(p_1+p_2)_\mu\frac{m_{F^*}^2}{m_{F^*}^2-q^2}I\equiv(p_1+p_2)_\mu G_V(q^2)I\ , \tag{18}$$

where G_V is a form factor describing the q^2 dependence of the coupling of the vector current to the $c\bar{s}$ hadronic state:

$$G_V(q^2)=\frac{m_{c\bar{s}}^2}{m_{c\bar{s}}^2-q^2} \tag{19}$$

and $m_{c\bar{s}}^2$ is the mass of the nearest vector meson with the hadron current quantum numbers. Following Wirbel, Stech, and Bauer[12] we introduce a factor I which in the quark model can be understood as the overlap integral between the initial and final meson wave functions. In the chiral SU(N) limit, $I=1$. Dominguez and Paver have estimated corresponding overlap factors for $c\bar{s}$, $c\bar{d}$, and $b\bar{u}$ transitions[13] using the QCD sum-rule technique. With suitable changes in the mass in G_V and the overlap integral the same expression, Eq. (18), describes

$$B^+\to\bar{D}^0+e^++\nu \quad\text{or}\quad B^0\to\pi^++e^-+\bar{\nu}\ .$$

The corresponding hadronic structure functions are

$$H_1=0,\ H_3=0,\quad H_2=\frac{m_1^2}{2\pi^3}|G_V I|^2\,\delta(p_2^2-m_2^2)\ . \tag{20}$$

[The expression $\delta(p_2^2-m_2^2)=(1/m_1^2)\delta(\mu^2-m_2^2/m_1^2)$ appears because the hadronic state is a single-particle state.] The total exclusive decay rate is given by

$$\Gamma=\frac{G_F^2 f(\theta_C)m_1^5}{32\pi^3}\int_0^{1-m_2^2/m_1^2}dx\int_0^{x[1-m_2^2/m_1^2/(1-x)]}dt\left[x\left[1-\frac{m_1^2}{m_1^2}-x\right]-t(1-x)\right]|G_V I|^2$$

$$=\frac{G_F^2 f(\theta)m_1^5}{192\pi^3}\int_0^{t_-}dt[(t-t_+)(t-t_-)]^{3/2}|G_V I|^2\ , \tag{21}$$

where

$$t_\pm=\frac{q_\pm^2}{m_1^2}=\left[\frac{m_1\pm m_2}{m_1}\right]^2 .$$

For the hadronic structure function corresponding to two pseudoscalars we consider, to be specific, the process

$$D^+\to K^-+\pi^++e^++\nu,\quad p_1\to p_2+p_3+k+k' .$$

The current-algebra threshold result in the limit of SU(4) symmetry is

$$J_\mu=\frac{2\sqrt{2}}{\pi^2F_\pi^3}\epsilon_{\mu\nu\alpha\beta}p_3^\nu p_2^\alpha p_1^\beta G_V(q^2)+\frac{2\sqrt{2}i}{3F_\pi}(2p_3+p_1-p_2)^\nu\left[g_{\mu\nu}G_V(q^2)-\frac{q_\mu q_\nu}{q^2-m_F^2}\right], \tag{22}$$

where the q^2 pole behavior corresponds to the graph of Fig. 1. The $q_\mu q_\nu$ terms which we shall now drop, have negligible contribution in the limit of vanishing lepton mass, where the lepton current is conserved. We now add resonance behavior in the two-body pseudoscalar channels, following the procedure of Chao *et al.*[9] (where the parameters $3\alpha f_V$ and $3\alpha f_A$ defined below were taken to be unity) as further developed in Ref. 10. The vector current is given by

$$J_\mu=\frac{2\sqrt{2}}{\pi^2F_\pi^3}\epsilon_{\mu\nu\alpha\beta}p_3^\nu p_2^\alpha p_1^\beta\frac{1}{2}\left[\frac{m_{D^*}^2}{m_{D^*}^2-s_{13}}+(1-3\alpha f_V)+3\alpha f_V\frac{m_{K^*}^2-im_{K^*}\Gamma}{m_{K^*}^2-s_{23}-im_{K^*}\Gamma}\right]G_V I \tag{23}$$

and the axial vector by

$$J_\mu=\frac{2\sqrt{2}i}{3F_\pi}\left\{(1-3\alpha f_A)(p_3-p_2)_\mu\right.$$

$$+3\alpha f_A\frac{m_{K^*}^2-im_{K^*}\Gamma}{m_{K^*}^2-s_{23}-im_{K^*}\Gamma_{K^*}}\left[(p_3-p_2)_\mu+(p_3+p_2)_\mu\frac{m_2^2-m_3^2}{m_{K^*}^2}\right.$$

$$\left.\left.+\frac{F_2^A(0)}{F_1^A(0)}p_{1\mu}\left[p_1(p_3-p_2)+p_1(p_3+p_2)\frac{m_2^2-m_3^2}{m_{K^*}^2}\right]\right]\right.$$

$$\left.+\frac{m_{D^*}^2}{m_{D^*}^2-s_{13}}(p_1+p_3)_\mu\right\}G_A I\ . \tag{24}$$

(In Ref. 9 the spin projection for the axial-vector part of the intermediate vector state was incomplete and the effect propagated into our subsequent formula for H_i. The effect is small on the numerical results of that paper, which did not account for the F_2^A form factor and used a much stronger vector form factor than is now believed correct.) In Eqs. (23) and (24) the introduction of the parameter α decouples the pole enhancement from the low-energy behavior. Without it, relations between different coupling constants evolve which are in disagreement with experiment. (For more discussion on this point see Ref. 10.) f_V and f_A parametrize the possibility that this decoupling is different for vector and axial-vector currents. I stands for overlap integrals, which are as-

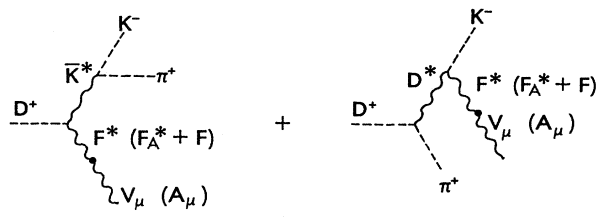

FIG. 1. Resonance-enhanced diagrams for $D\to K\pi e\nu$. K^* and D^* dominate the $K\pi$ and $D\pi$ channels, respectively. The vector- and axial-vector-current channels are enhanced by the vector, axial-vector, and pseudoscalar hadrons with the appropriate flavor.

sumed to be equal for the vector and axial-vector current. In the chiral-symmetry limit Eqs. (23) and (24) reduce to Eq. (22) when s_{13} and s_{23} are evaluated at soft threshold $s_{13}=s_{23}=0$ and $m_2=m_3=0$ for any values of the parameter αf_V and αf_A. We shall treat the slowly varying distant pole contribution in the 13 channel by evaluating these terms at current-algebra threshold $s_{13}=0$. Otherwise it would have been necessary to modify the pole term in the 13 channel in the same way as the 23 channel with threshold behavior and pole enhancement decoupled. This way this term becomes part of the contact term. These contact terms along with terms proportional to $(1-3\alpha f_{V,A})$ describe small constant terms required by current algebra. Even far from the chiral-symmetry limit they may represent nonresonant background underneath the resonant terms or the accumulated effect of higher resonances, as discussed below. We notice that the terms proportional to F_2^A are irrelevant at the threshold point. Therefore they do not lead to a modification of the contact term.

In narrow width approximation, for $D\to K^*e\nu$ where only the K^* intermediate state is important, we can relate our form factor to $D\to K^*$ transition factors, as they appear in the literature:[8]

$$\langle K^*(p)|J_\mu|D(p_1)\rangle = e_\nu^*(F_1^A g_\mu^\nu + F_2^A p_{1\mu}p_1^\nu + iF^V\epsilon_{\mu\nu\rho\sigma}p_1^\rho p^\sigma)\ . \quad (25)$$

The correspondence between the form factors is

$$3\alpha f_V I G_V = \sqrt{2}g_{\bar{K}^{*0}K^-\pi^+}F^V(0)G_V\frac{\pi^2F_\pi^3}{m_{K^*}^2}\equiv C_V\ , \quad (26)$$

$$3\alpha f_A I G_A = \sqrt{2}g_{\bar{K}^{*0}K^-\pi^+}F_1^A(0)G_A\frac{3F_\pi}{4m_{K^*}^2}\equiv C_A\ . \quad (27)$$

An early discussion of the behavior of $F^V(0)$, $F_1^A(0)$, and $F_2^A(0)$ in the quark model was given by Ali *et al.*[14] Körner and Schuler[11] have taken this up and match the spin properties of the mesonic transitions to the free quark decay transitions at $q^2=0$, obtaining the relations

$$F_1^A(0)=(m_1+m_X)I\ ,$$
$$F_2^A(0)=\frac{-2}{m_1+m_X}I\ , \quad (28)$$
$$F^V(0)=\frac{2}{m_1+m_X}I\ ,$$

where m_1 is the decaying meson mass and m_X is the vector-meson hadronic final-state mass. [We have taken the sign of F^V here for $D\to K^*$ semileptonic decay; for $B\to K^*$ semileptonic decay, $F^V(0)$ changes sign.] The effect is seen in the $F^V(0)F_1^A(0)$ interference term which for D (B) decay is positive (negative) at low electron momentum and negative (positive) at high electron momentum in $d\Gamma/dE_e$.

Overlap factors have been estimated by several authors. Körner and Schuler[11] take a common factor $I=0.7$ for the $b\to c$ transition form factor, following Wirbel, Stech, and Bauer,[12] who use an infinite-momentum-frame quark model to estimate $I=0.71$, 0.65, and 0.69 for overlap factors multiplying F^V, F_1^A, and F_2^A, respectively, when the average transverse quark momentum is 0.400 GeV. In a refined analysis of overlap factors for semileptonic B and D decays, Bauer and Wirbel[8] find possible variations of overlap factors for F_V, F_1^A, and F_2^A in the ranges 0.92–0.35, 0.85–0.33, and 1.12–(−0.04) respectively for B decays to D^* mesons and 1.65–0.63, 1.14–0.44, and 1.89–(−0.10) for D mesons to K^* mesons, using monopole form factors. This range can be regarded as some measure of the theoretical uncertainty in estimating overlaps for the underlying dynamics. Of course, one has to keep in mind that these results for the overlap factors in the framework of the infinite-momentum-frame quark model[12] or the quark potential model[3,8] come from model calculations and are purely phenomenological. They only give us indications of the values of these parameters. The same holds for the Körner-Schuler relations, Eqs. (28). All these form factors should be determined experimentally. If this is done we shall have better confidence in the validity of the various quark-model results referred to above.

As mentioned in the Introduction, perturbative QCD calculations for inclusive decays would seem to be an attractive escape from the uncertainties involved with the nonperturbative physics of exclusive processes. Recently, however, Isgur, Scora, Grinstein, and Wise[3] have criticized the usual free quark model concerning the shape and end-point spectrum of heavy-quark inclusive semileptonic decay and argued the need for detailed nonperturbative analysis of dominant exclusive channels, especially concerning the end-point spectrum. They are thus in harmony with earlier literature studying exclusive channels using predictions of nonperturbative, phenomenological models. They point out the wide range of predictions of these models, consistent with the range of overlap integrals mentioned above. It is not the purpose of this paper to add more predictions in this respect. Instead we take the attitude of first fixing F^V, F_1^A, and F_2^A according to Eq. (28) and then studying the consequences of changes of these parameters in the vicinity of their fiducial values. We treat the overlap parameter I similarly. As we mentioned in the Introduction our next objective is to study backgrounds beneath these states and the accuracy of the narrow-width approximation, a task for which our formalism is uniquely suited. Though we will present results for both full two-body kinematics and the narrow-width approximation, the formulas for H_1, H_2, and H_3 shall be now written down in the narrow-width approximation because they are too lengthy in the general case.

They shall be written in terms of the parameters

$$\gamma_1=\frac{1}{2}\frac{m_2^2-m_3^2}{m_{K^*}^2}\ , \quad (29)$$

$$\gamma_2=\frac{F_2^A}{4F_1^A s_{23}}\lambda^{1/2}(s_{23},m_1^2,q^2)\lambda^{1/2}(s_{23},m_2^2,m_3^2)\ , \tag{30}$$

$$C=\frac{\lambda^{1/2}(s_{23},m_2^2,m_3^2)}{4(2\pi)^5 s_{23}}\ . \tag{31}$$

In the narrow-width approximation s_{23} is evaluated at the resonance mass:

$$s_{23}=\mu^2 m_1^2=m_{K^*}^2\ . \tag{32}$$

Then we get

$$H_1=\lambda(s_{23},m_2^2,m_3^2)\frac{C}{3s_{23}}\frac{m_{K^*}^3}{\Gamma_{K^*}}\delta(s_{23}-m_{K^*}^2)\left[\frac{|C_V|^2\lambda(s_{23},m_1^2,q^2)}{8\pi^3F_\pi^6}+\frac{8\pi}{9F_\pi^2}|C_A|^2\right], \tag{33}$$

$$\begin{aligned}H_2=\frac{C}{3s_{23}^2}\frac{m_{K^*}^3}{\Gamma_{K^*}}\delta(s_{23}-m_{K^*}^2)m_1^2\Bigg[&-s_{23}|C_V|^2\frac{2}{2\pi^3F_\pi^6}\lambda(s_{23},m_2^2,m_3^2)q^2\\&+|C_A|^2\frac{8\pi}{9F_\pi^2}\Bigg[\lambda(s_{23},m_2^2,m_3^2)+12s_{23}^2(\gamma_1^2+\tfrac{1}{3}\gamma_2^2)+3(m_2^2-m_3^2)^2\\&-12s_{23}(m_2^2-m_3^2)\gamma_1-4s_{23}\gamma_2(s_{23}-m_1^2+q^2)\frac{\lambda^{1/2}(s_{23},m_2^2,m_3^2)}{\lambda^{1/2}(s_{23},m_1^2,q^2)}\Bigg]\Bigg],\end{aligned} \tag{34}$$

$$H_3=C_VC_A\frac{4}{3\pi F_\pi^4}\frac{\lambda(s_{23},m_2^2,m_3^2)}{3s_{23}}\frac{m_{K^*}^3}{\Gamma_{K^*}}\delta(s_{23}-m_{K^*}^2)Cm_1^2\ . \tag{35}$$

These equations for H_1, H_2, and H_3 agree with the equations for these structure functions in Ref. 9, if $3\alpha f_{V,A}=1$ and $\gamma_1=\gamma_2=0$. γ_2 parametrizes the contribution of the new form factor F_2^A, which is irrelevant for the low-energy behavior. γ_1 appears because we have built in the correct propagator for the intermediate vector state. We see that all terms proportional to $m_2^2-m_3^2$ cancel. From these structure functions we obtain the helicity structure functions introduced in Eq. (12):

$$\Delta^2H_\pm=\lambda(s_{23},m_2^2,m_3^2)\frac{C}{3s_{23}}\frac{m_{K^*}^3}{\Gamma_{K^*}}\delta(s_{23}-m_{K^*}^2)\frac{\pi}{2}\times\left[\frac{\pm C_V\lambda^{1/2}(s_{23},m_1^2,q^2)}{2\pi^2F_\pi^3}+\frac{4C_A}{3F_\pi}\right]^2, \tag{36}$$

$$\begin{aligned}\Delta^2H_0=\lambda(s_{23},m_2^2,m_3^2)&\frac{C}{12m_1^2s_{23}^2}\frac{m_{K^*}^3}{\Gamma_{K^*}}\delta(s_{23}-m_{K^*}^2)\frac{\pi}{2}\\&\times\frac{16}{9F_\pi^2}|C_A|^2\left[(m_1^2-s_{23}-q^2)+\lambda(q^2,s_{23},m_1^2)\frac{F_2^A}{2F_1^A}\right]^2.\end{aligned} \tag{37}$$

We may now substitute $H_\pm$ and H_0 into Eq. (14) and perform the μ^2 integration. Then the first two terms correspond to the transversely polarized K^* and the last term corresponds to the longitudinally polarized K^*. This equation agrees with the corresponding equation in Ref. 11 if we substitute the relations (26) and (27) and use the well-known formula for the K^* width.

III. NUMERICAL RESULTS

In presenting our results we shall take as input the weak mixing matrix elements when they are reliably known from lifetime measurements. Our objects of study are overlap integrals, weak mixing angles for $b\to u$ transitions, and the effects of current-algebra contact terms and the narrow-width approximation on extracting these parameters.

$D\to Ke\nu$. For D decays to strange states we take $|V_{cs}|=0.974$. Then from the decays $D^0\to K^-+e^++\nu$ and $D^+\to\bar{K}^0+e^++\nu$, using the monopole form factor with mass $m_{c\bar{s}}=2.114$ GeV we find

$$\Gamma(D\to Ke\nu)=|V_{cs}I|^2\times 10.27\times 10^{-14}\ \text{GeV}\ . \tag{38}$$

Taking the measured values from the E691 experiment at Fermilab,[5,15]

$$\begin{aligned}\Gamma(D^0\to K^-+e^++\nu)&=(6.0\pm1.2)\times10^{-14}\ \text{GeV}\ ,\\ \Gamma(D^+\to\bar{K}^0+e^++\nu)&=(6.3\pm1.3)\times10^{-14}\ \text{GeV}\ ,\end{aligned} \tag{39}$$

or from the Mark III experiment at SLAC (Ref. 15),

$$\begin{aligned}\Gamma(D^0\to K^-+e^++\nu)&=(6.5\pm1.1)\times10^{-14}\ \text{GeV}\ ,\\ \Gamma(D^+\to\bar{K}^0+e^++\nu)&=(4.5\pm1.3)\times10^{-14}\ \text{GeV}\ ,\end{aligned} \tag{40}$$

we determine the overlap integrals from these data. The result is

$$\begin{aligned}&\text{E691},\ D^0\text{:}\ I=0.78\pm0.08;\ D^+\text{:}\ I=0.80\pm0.07\ ,\\ &\text{Mark III},\ D^0\text{:}\ I=0.82\pm0.06;\ D^+\text{:}\ I=0.68\pm0.09\ .\end{aligned} \tag{41}$$

The average value is $I=0.77\pm0.04$. This is in good

agreement with the theoretical values that Wirbel, Stech, and Bauer obtain in their infinite-momentum-frame approach, $I=0.76\pm0.06$ (Ref. 12), and Dominguez and Paver get from QCD sum rules, $I=0.75\pm0.05$ (Ref. 13). We consider therefore that the value $I=0.7$ is a good choice for overlap integrals, which we will use as a universal value for D and B transitions. We also remark that in the E691 experiment the form-factor mass has been determined from the data with the result $m_{c\bar{s}}=2.1\pm0.3$ GeV, in agreement with the assumed value above.

$D\to\pi e\nu$, $\eta e\nu$, $\eta' e\nu$. For D decays to π, η, and η', using an η,η' mixing angle of $-11°$, we find the relative couplings

$$\frac{D^+}{\sqrt{2}}(\pi^0-0.71\eta-0.70\eta')+D^0\pi^+$$

and the rates

$$\begin{aligned}\Gamma(D^+\to\pi^0+e^++\nu)&=|V_{cd}I|^2\times1.005\times10^{-13}\text{ GeV},\\ \Gamma(D^+\to\eta+e^++\nu)&=|V_{cd}I|^2\times0.231\times10^{-13}\text{ GeV},\\ \Gamma(D^+\to\eta'+e^++\nu)&=|V_{cd}I|^2\times0.053\times10^{-13}\text{ GeV},\end{aligned}\tag{42}$$

where we use the form-factor mass $m_{c\bar{d}}=2.01$ GeV. If we use the same overlap integral $|I|\approx0.7$ found in $D\to Ke\nu$ and $|V_{cd}|=0.222$ we find

$$\begin{aligned}\Gamma(D^+\to\pi^0e^+\nu)&=\Gamma(D^0\to\pi^-e^+\nu)/2\\ &=0.243\times10^{-14}\text{ GeV},\\ \Gamma(D^+\to\eta e^+\nu)&=0.558\times10^{-15}\text{ GeV},\\ \Gamma(D^+\to\eta' e^+\nu)&=1.28\times10^{-16}\text{ GeV}.\end{aligned}\tag{43}$$

The one-pion transition has been observed,[15]

$$\Gamma(D^0\to\pi^-e^+\nu)=(0.62\pm0.36)\times10^{-14}\text{ GeV},\tag{44}$$

and corresponds to an overlap integral $I=0.79\pm0.20$

Thus a reasonably clear, consensus picture of semileptonic decays of the D meson to a single pseudoscalar emerges when these results are compared to the related work of Dominguez and Paver,[13] and the overlap integral analysis of Wirbel, Stech, and Bauer.[8] We shall see whether this consensus survives when B decays to a single pseudoscalar are studied below.

$D\to K\pi e\nu$ ($D\to K^*e\nu$). Before that we turn to the decay of D to two-body resonance states K^* and ρ. Our formalism allows us to study the resonance cases: (1) two-body kinematics with contact terms, (2) two-body kinematics without contact terms, and (3) the narrow-width approximation (no contact terms). We shall also present results for the decay rate to longitudinal and transversely polarized K^*'s.

We first consider $D^+\to(K^-\pi^+e^+\nu+\bar{K}^0\pi^0e^+\nu)$ and $(D^+\to\bar{K}^{0*}e^+\nu)$ and to be specific use $I=0.7$, $|V_{cs}|=0.974$, the form-factor mass $m_{c\bar{s}}=2.114$ GeV, and the form-factor parametrization of Körner and Schuler, as given in Eq. (28) of the preceding section. The results are

$$\begin{aligned}&\Gamma=4.42\times10^{-14}\text{ GeV}\\ &\qquad\text{(two-body kinematics with contact terms)},\\ &\Gamma=4.15\times10^{-14}\text{ GeV}\\ &\qquad\text{(two-body kinematics without contact terms)},\\ &\Gamma=4.59\times10^{-14}\text{ GeV}\\ &\text{(narrow-width approximation without contact terms)}.\end{aligned}\tag{45}$$

The effect of the narrow-width approximation is to increase the rate by 11% over the corresponding calculation using full two-body kinematics with no contact term. The effect of the contact terms is to increase the rate by 7% over the corresponding two-body calculation without contacts. The electron decay spectra for each case is shown in Fig. 2. It is clear that we are dealing here with small effects but it is interesting to note that the contact term, equivalent to a constant nonresonant background, is in rough agreement with that data as reported by Morrison.[15] In the E691 experiment the nonresonant background in the D^0 and in the D^+ transition is of the order of 10%, with, however, rather large experimental errors. The Mark III experiment claims to have found rather large nonresonant contributions. The ratio of nonresonant to resonant branching ratio is here roughly 1:2.

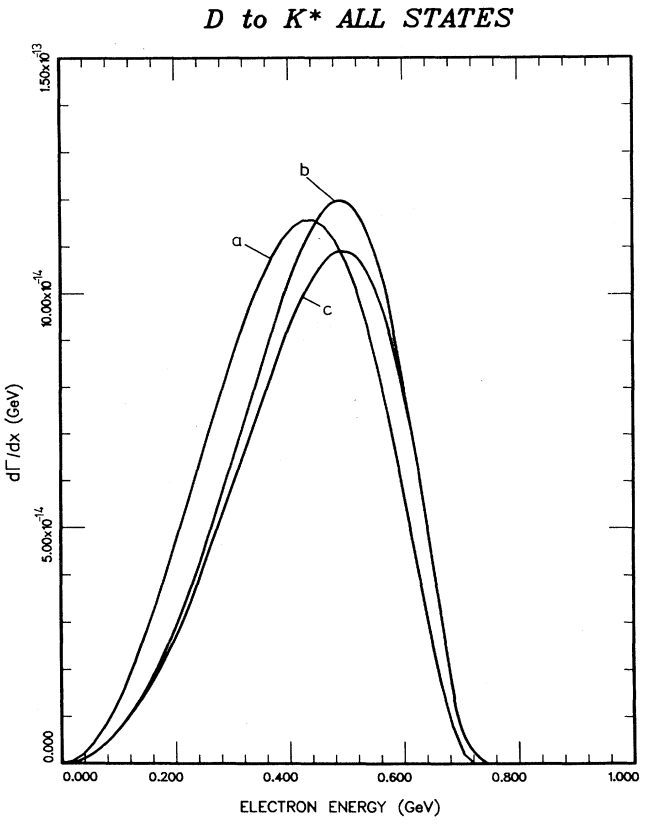

FIG. 2. Electron spectrum for D^+ semileptonic decay to πK. (a) narrow-width approximation. (b) two-body kinematics *with* contact terms. (c) two-body kinematics *without* contact terms.

As seen above in our model the nonresonant terms increase the partial width by 7%.

Having determined the effects of contact terms and the narrow-width approximation in $D \to K\pi$ semileptonic decay we now study the variation of the decay rate and spectrum with respect to the form factors F^V, F_1^A, and F_2^A. We will vary the ratio $F_2^A/F_1^A \equiv -2R/(m_D + m_{K^*})^2$ from $R=2$ to -2 and allow F^V to take on the values 0, F^V, and $2F^V$, where F^V is given by Eq. (28). By adjusting F_1^A the rate can be made to fit the experimental value. The results will be presented as curves with a common (unit) area, to illustrate how the electron spectrum shape changes. Figure 3 shows how the spectral shapes change as F_2^A/F_1^A varies from -5 to $+5$. The *shape* change is not dramatic, although the decay *rate* itself (if not adjusted by scaling F_1^A) changes by a factor of 3.3, as shown in Table I, if R is varied only between -2 and 2.

Similarly, we can vary F^V for fixed F_2^A and F_1^A. The results, normalized to constant area, are shown in Fig. 4 and Table I. (The change in the absolute rate in this case is also slight because the vector contribution is such a small fraction of the total rate.) The shape of the spectrum changes to some extent although the vector contribution is small. If F^V is decreased to zero the maximum of the spectrum shifts nearer to the end point.

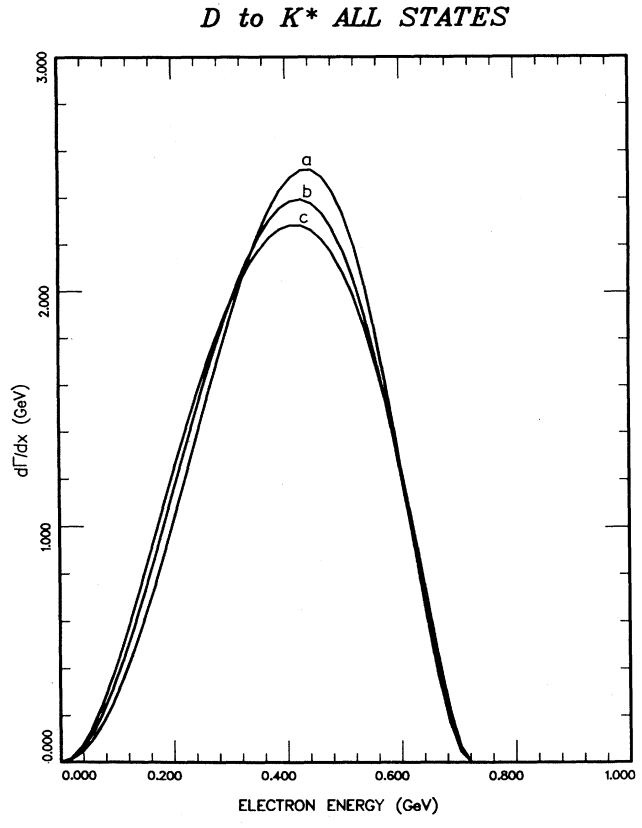

FIG. 3. Electron spectrum for $D \to K^* e\nu$ for various values of R, where $F_2^A/F_1^A = -2R/(m_B + m_{D^*})^2$. The curves have been adjusted to have a common area. (a) $R=1$, (b) $R=5$, (c) $R=-5$.

TABLE I. Decay rate for $D^+ \to \bar{K}^{0*}\nu$ for various values of R, where $F_2^A/F_1^A = -2R/(m_D + m_{K^*})^2$, and various values of $F^V=0$, $F^V=F^V$ [Eq. (28)], and $F^V=2F^V$ [Eq. (28)]. The last column is the asymmetry parameter which appears in the angular distribution $1+\alpha\cos^2\theta$ of the K momentum relative to the K^* in the center-of-mass system of the leptons. The last row is the decay rate for transversely polarized K^* mesons.

R	$\Gamma(F^V=0)$ (10^{-14} GeV)	$\Gamma(F^V)$ (10^{-14} GeV)	$\Gamma(2F^V)$ (10^{-14} GeV)	$\alpha(F^V)$
2.0	3.30	3.40	3.69	0.183
1.0	4.49	4.59	4.88	1.30
0.5	5.29	5.39	5.68	2.05
0	6.23	6.32	6.62	2.93
−0.5	7.30	7.39	7.69	3.93
−1.0	8.50	8.60	8.89	5.06
−2.0	11.3	11.4	11.7	7.70
Γ_T	2.04	2.13	2.43	

Also shown in Table I is the transverse decay rate and the corresponding value of the asymmetry parameter

$$\alpha = \frac{2\Gamma_L}{\Gamma_T} - 1 \tag{46}$$

which appears in the angular distribution $1+\alpha\cos^2\theta$ of the K momentum relative to the K^* in the center-of-mass system of the leptons. This parameter *is* sensitive to the

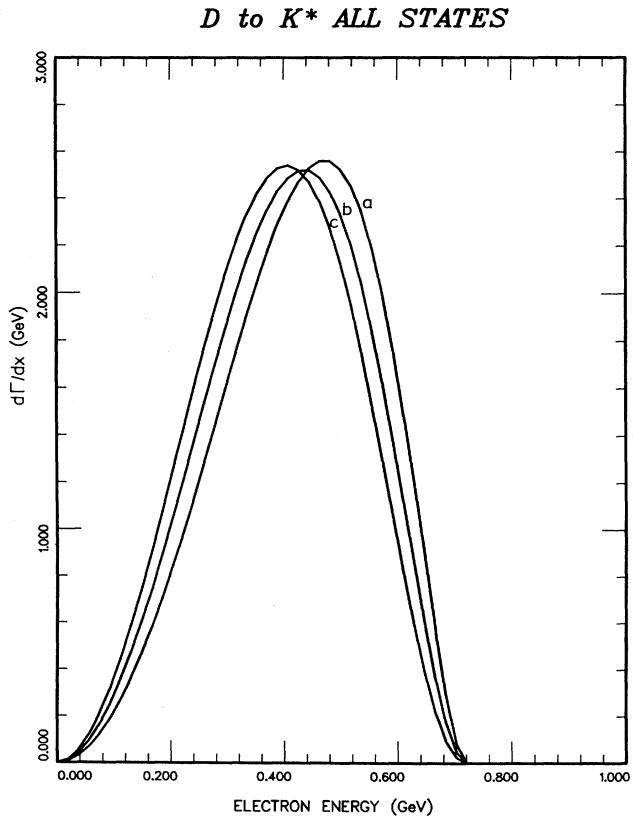

FIG. 4. Electron spectrum for $D \to K^* e\nu$ for various values of F^V. The curves have been adjusted to a common area. (a) $F^V=0$, (b) $F^V=F^V$ [Eq. (28)], (c) $F^V=2F^V$ [Eq. (28)].

F_2^A/F_1^A ratio, as shown in Table I. It has been evaluated at the central value of F^V.

The experimental data with which we can compare come again from the Mark III Collaboration and the E691 experiment. Since the Mark III data show an appreciable nonresonant background in contrast with our model, we compare only to the E691 (Ref. 15) data, which are consistent with our results with respect to the nonresonant contribution.[16] These results are $\Gamma(D^0\to K^-{}^*e^+\nu)=(2.62\pm0.56)\times10^{-14}$ GeV, the nonresonant background is $(0.31\pm0.22)\times10^{-14}$ GeV. The partial width $\Gamma(D^+\to K^{0*}e^+\nu)=(2.83\pm0.54)\times10^{-14}$ GeV, with nonresonant background $(0.32\pm0.25)\times10^{-14}$ GeV. So the D^+ and the D^0 decays have comparable rates. The average, including the 10% background, is equal to $(3.07\pm0.32)\times10^{-14}$ GeV. Another data set is the recently measured K^*-decay angular distribution. The result quoted is $\Gamma_L/\Gamma_T=[2.4+1.7(-0.9)\pm0.2]$. This means that the K^* is strongly longitudinally polarized. Because of the large error the parameter R could still lie between -2.0 and 1.0, as can be seen from Table I. If we assume that Γ_L/Γ_T has its central value 2.4, then $R=-0.4$ and from the rate we can determine the overlap factor I with the result that $I=0.42\pm0.02$ [we took the result from $\Gamma(FV)$ in Table I] instead of $I=0.7$, which was assumed to generate the numbers in Table I. With better data for α and good measurements of the electron spectrum for the K^* channel it will eventually be possible to pin down the three form factors F^V, F_1^A, and F_2^A.

$D\to\pi\pi e\nu$ ($D\to\rho e\nu$). As in the $K\pi$ case, we study $D\to\pi\pi e\nu$ ($D^-\to\rho^0 e\nu$) with ρ pole in the $\pi\pi$ channel to examine effects of the contact terms and the narrow-width approximation. To be specific and for comparisons with $B\to\pi\pi e\nu$ ($B\to\rho e\nu$) we present our results in terms of the overlap integrals $I=0.33$ and $I=0.7$, discussed in the $B\to\pi\pi$ section, and still using $V_{cd}=0.222$. The results are, for $I=0.33$,

$$\Gamma=3.98\times10^{-16}\text{ GeV}$$

(two-body kinematics, no contact term),

$$\Gamma=4.64\times10^{-16}\text{ GeV}$$

(narrow-width approximation, no contact term), (47)

$$\Gamma=6.13\times10^{-16}\text{ GeV}$$

(two-body kinematics with contact terms);

and for $I=0.7$,

$$\Gamma=3.98\times10^{-16}\text{ GeV}$$

(two-body kinematics, no contact term),

$$\Gamma=20.9\times10^{-16}\text{ GeV}$$

(narrow-width approximation, no contacts terms), (48)

$$\Gamma=19.5\times10^{-16}\text{ GeV}$$

(two-body kinematics with contact terms).

First we discuss the $I=0.33$ calculation, where the contact terms are relatively more important because the resonance term is more sharply damped by the overlap factor. As before, the narrow-width approximation overestimates the resonance rate (no contact terms), now by 17%, but by far the larger effect is that of the contact terms, which enhance the rate by about 54%, when $I=0.33$. The contact terms are *relatively* more important here because they contribute to the $\pi\pi$ amplitude roughly the *same* as in $D\to K\pi e\nu$ whereas the resonance contribution is *less* because it is of order $I(m/\Gamma)$, which is 1.68 for ρ and 12.25 for K^*. If contact terms are present at the magnitude suggested by chiral SU(4)—admittedly a badly broken symmetry but perhaps useful for estimating rough magnitudes—then they will clearly have significant effects on the analysis of $D\to\rho e\nu$. As in the $K\pi$ case they may be evidenced by large backgrounds beneath the ρ resonance. For their effect on the electron spectrum, see Fig. 5. When the larger overlap, $I=0.7$, is taken, the effects are less dramatic, as expected.

Such direct couplings of the current to three pseudoscalars (here $D\pi\pi$) have been discussed by Braaten *et al.*[17] and by two of us[10] in connection with $\rho^-\to\pi^-\gamma$, $\omega\to3\pi$, $\omega\to\pi^0\gamma$, and $\omega\to\pi^0\mu^+\mu^-$. The contact terms also have an interpretation in the framework of generalized vector dominance where they model the sum of higher mass resonance terms where masses are large com-

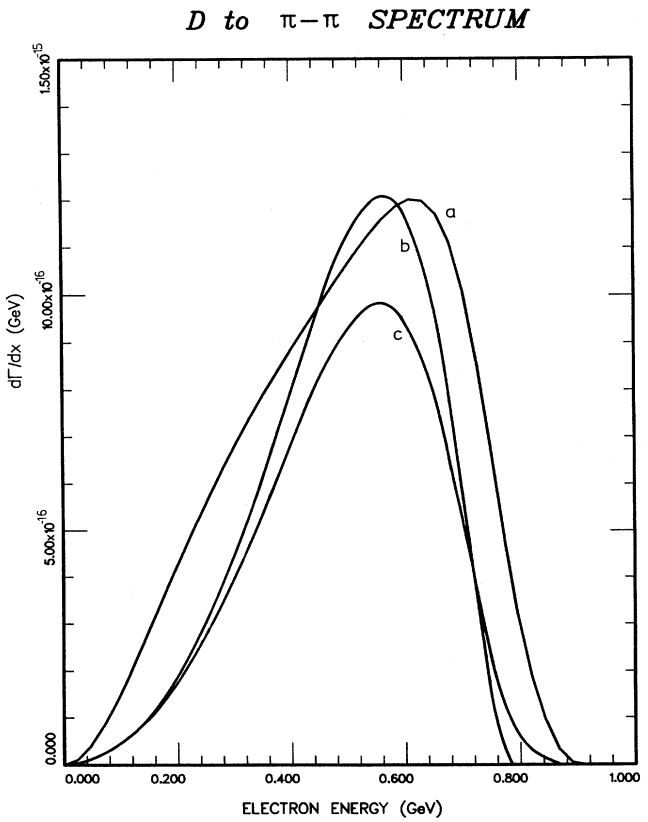

FIG. 5. Electron spectrum for $D^-\to\pi^+\pi^-e\nu$ ($D^-\to\rho^0 e\nu$): (a) two-body kinematics *with* contact terms, (b) narrow-width approximation, (c) two-body kinematics *without* contact terms.

pared to the $\pi\pi$ energy. (For an application of such higher resonances to vector-meson decays in the framework of the dual model see Dominguez.[18])

$B \to De\nu$. We find

$$\Gamma(B^- \to \bar{D}^0 e\nu) = |V_{cb} I|^2 \times 1.21 \times 10^{-11} \text{ GeV} , \quad (49)$$

where we have used a form-factor mass $m_{b\bar{c}} = 6.340$ GeV. Using $|V_{cb}| = 0.045$ we find the estimate[12] $I \sim 0.7$ corresponds to an exclusive rate $\Gamma(B^- \to \bar{D}^0 e\nu) = 1.20 \times 10^{-14}$ GeV. We shall continue to use $I = 0.7$ below to present our results.

$B^- \to D\pi e\nu$ ($B^- \to D^{0*} e\nu$). We treat $B^- \to \bar{D}^{0*} e\nu$ only in the narrow-width approximation, where the rate we find is

$$\Gamma(B^- \to \bar{D}^{0*} e\nu) = |V_{cb} I|^2 \times 3.61 \times 10^{-11} \text{ GeV} . \quad (50)$$

Again we test for variation with F^V and F_2^A/F_1^A by varying R in $F_2^A/F_1^A = -2R/(m_{D^*} + m_B)^2$ between 5 and -5 and allowing F^V to take on the values 0, F^V, and $2F^V$, where F^V is given in Eq. (28). The results, along with the transverse decay rate Γ_T and the asymmetry parameter α, are given in Table II and presented in Figs. 6 and 7. Table II is based on $|V_{cb}| = 0.045$ and $I = 0.7$. Figures 6 and 7 are normalized to unit area to show how the shape changes with variations in F^V and F_2^A/F_1^A. Increasing F^V and the ratio R shifts the decay spectrum to higher electron energy. It is again notable how sensitive the α asymmetry parameter is to F_2^A/F_1^A. This experimental measurement yields very useful constraints on the determination of the form factors. The experimental situation is as follows. The B lifetime is $(1.18 \pm 0.14) \times 10^{-12}$ sec

TABLE II. Decay rate for $B^- \to D^{0*} e\nu$ for various values of R, where $F_2^A/F_1^A = -2R/(m_B + m_{D^*})^2$ and various values of F^V ($F^V = 0$, $F^V = F^V$ [Eq. (28)] and $F^V = 2F^V$ [Eq. (28)]). The last column is the asymmetry parameter which appears in the angular distribution $1 + \alpha \cos^2\theta$ of the D momentum relative to the D^* in the center-of-mass system of the leptons. The last row is the decay rate for transversely polarized D^* mesons.

Ratio R	$\Gamma(F^V = 0)$ (10^{-14} GeV)	$\Gamma(F^V)$ (10^{-14} GeV)	$\Gamma(2F^V)$ (10^{-14} GeV)	$\alpha(F^V)$
5.0	3.87	3.99	4.33	1.77
2.0	2.29	2.41	2.75	−0.120
1.0	3.47	3.58	3.93	1.28
0.5	4.38	4.49	4.84	2.38
0	5.50	5.61	5.96	3.71
−0.5	6.83	6.95	7.29	5.31
−1.0	8.38	8.49	8.84	7.16
−2.0	12.1	12.2	12.5	11.6
−5.0	28.4	28.5	28.9	31.1
Γ_T	1.56	1.67	2.02	

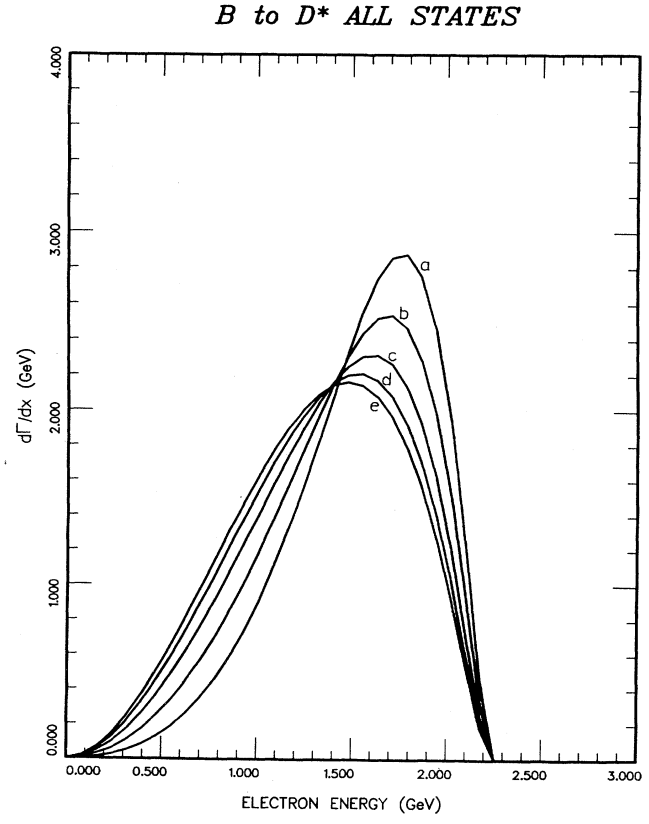

FIG. 6. Electron spectrum for $B \to D^* e\nu$ for various values of R, where $F_A^2/F_A^1 = -2R/(m_B + m_{D^*})^2$. The curves have been adjusted to have a common area. (a) $R = 2$, (b) $R = 1$, (c) $R = 0$, (d) $R = -1$, (e) $R = -2$.

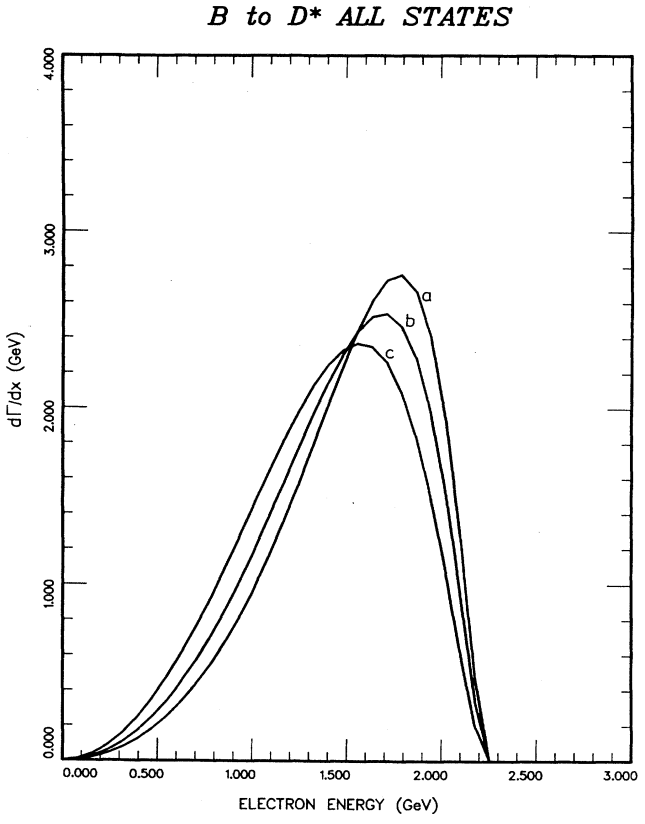

FIG. 7. Electron spectrum for $B \to D^* e\nu$ for various values of F^V. The curves have been adjusted to have a common area. (a) $F^V = 2F^V$ [Eq. (28)], (b) $F^V = F^V$ [Eq. (28)], (c) $F^V = 0$.

(world average).[4] The semileptonic branching ratio to D^* has been measured by the Argus Collaboration at DESY with the result $B(B^0\to D^* e\nu)=(7.0\pm1.2\pm1.9)\%$.[4] The world average of the total semileptonic branching ratio is $(11.8\pm0.7)\%$.[4] It is reasonable to assume that the D and the D^* channel dominate the semileptonic decay of the B's. Then the branching fraction to $De\nu$ is $(4.8\pm2.4)\%$ and D and D^* are 41% and 59% of the total semileptonic decay. Furthermore the α parameter has been measured as $\alpha=0.3\pm0.6\pm0.3$ (Ref. 4) and $\alpha=0.7\pm0.9$ (Ref. 19). The experimental width $B\to D^* e\nu=(3.90\pm1.25)\times10^{-14}$ GeV can be compared with our results in Table II. The α parameter comes out right if $R\sim1.5$ and I is increased to $I=0.8$. [We note that also the transition to single D's needs a larger overlap than 0.7 since experimentally $\Gamma(B\to De\nu)=(2.68\pm1.34)\times10^{-14}$ GeV, which is more than a factor of 2 larger than the theoretical value with $I=0.7$.] We remark that Körner and Schuler[8] have obtained somewhat different results since they assumed dipole form factors for F^V and F_2^A. Since the masses for such dipole form factors are even less known than for the monopole form factors, we preferred to work with monopoles only.

$B\to\pi e\nu$. We find

$$\Gamma(B^-\to\pi^0 e^-\nu)=\Gamma(B^0\to\pi^+ e\nu)/2 =|V_{ub}I|^2\times2.19\times10^{-11}\ \text{GeV} \quad (51)$$

using the form-factor masses

$$m_{b\bar{u}}=5.324\ \text{GeV}$$

in G_V. If we test for sensitivity to G_V by using a dipole instead of a monopole form factor we find the result

$$\Gamma(B^-\to\pi^0 e^-\nu)=\Gamma(B^0\to\pi^+ e\nu)/2 =|V_{ub}I|^2\times8.52\times10^{-11}\ \text{GeV} \quad (52)$$

with a spectrum very sharply peaked at the end point. The two spectra are shown in Fig. 8. The sensitivity of the spectrum to the dipole mass is illustrated by showing also the result for a dipole mass of 5.916 GeV. Of course we have no theoretical reason to assume a dipole form factor at this place with the mass value given above. A better way would be to assume generalized vector-dominance form factors, where the smallest intermediate mass is the mass we have used above.[18]

We can also express these results as branching ratios, using 1.18×10^{-12} sec for the B lifetime as reported by Schröder,[4]

$$B(B^0\to\pi^+ e\nu)=\begin{cases}79|V_{ub}I|^2, & \text{monopole form factor,}\\ 305|V_{ub}I|^2, & \text{dipole form factor.}\end{cases} \quad (53)$$

These may be compared with recent CLEO results[20]

$$B(B\to\pi^+ e\nu)<2.5\times10^{-4} \quad (54)$$

and yield the limits

$$|V_{ub}I|<1.78\times10^{-3},\ \text{monopole form factor},\qquad |V_{ub}I|<0.905\times10^{-3},\ \text{dipole form factor}. \quad (55)$$

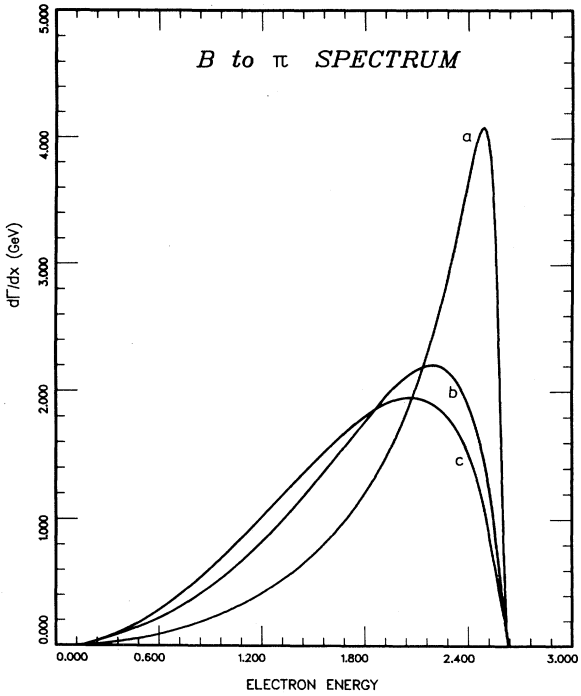

FIG. 8. Electron spectrum for $B\to\pi e\nu$ for various vector form factors. The curves have been adjusted to have a common area (a) dipole form factor with mass $m_{b\bar{u}}=5.324$ GeV, (b) monopole form factor with same mass as in (a), (c) dipole form factor with mass $m_{b\bar{u}}=5.916$ GeV.

$B\to\pi\pi e\nu$ ($B^-\to\rho^0 e^-\nu$). For the narrow-width approximation we find

$$\Gamma=|V_{ub}I|^2\times1.29\times10^{-10}\ \text{GeV},\ \text{monopole form factor},\qquad \Gamma=|V_{ub}I|^2\times1.00\times10^{-10}\ \text{GeV},\ \text{dipole form factor}. \quad (56)$$

While the widths are quite similar, the dipole form factor shifts the spectrum sharply to higher electron momentum, as shown in Fig. 9. These results can also be expressed as branching ratios using the lifetime quoted above:

$$B(B^-\to\rho^0 e^-\nu)=\begin{cases}232|V_{ub}I|^2, & \text{monopole form factor,}\\ 179|V_{ub}I|^2, & \text{dipole form factor.}\end{cases} \quad (57)$$

These may be compared to recent CLEO results[20]

$$B(B^-\to\rho^0 e\nu)<3.0\times10^{-4} \quad (58)$$

and yield the limits

$$|V_{ub}I|<1.14\times10^{-3},\ \text{monopole form factor},\qquad |V_{ub}I|<1.29\times10^{-3},\ \text{dipole form factor}. \quad (59)$$

As we expect $|I|>0.25$, this would imply that $|V_{ub}/V_{cb}|<0.1$.

To investigate effects of two-body kinematics and contact terms we use the overlap factor $I=0.33$ and express our results in terms of $|V_{ub}|^2$. They are, for $I=0.33$ and a monopole form factor,

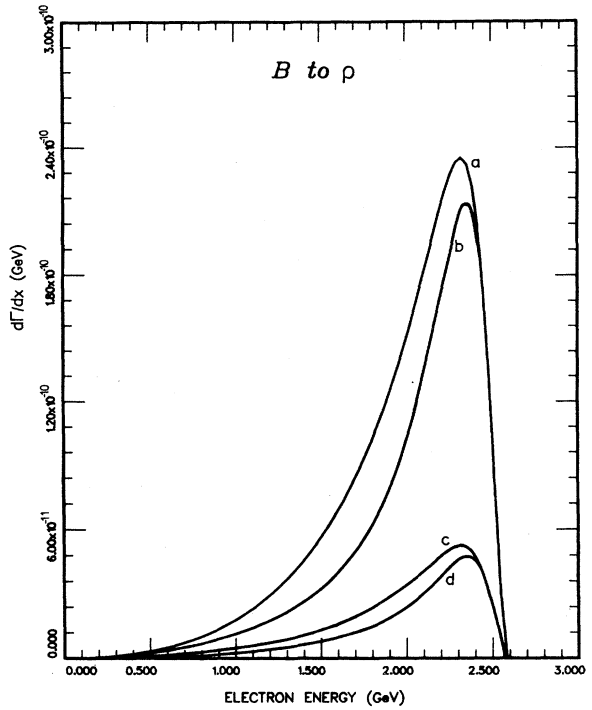

FIG. 9. Electron spectrum for $B \to \rho^0 e \nu$ for overlap integrals $I=0.7$ and 0.33 and monopole and dipole form factors: (a) $I=0.7$, monopole form factor; (b) $I=0.7$, dipole form factor; (c) $I=0.33$, monopole form factor; (d) $I=0.33$, dipole form factor.

$$\Gamma = |V_{ub}|^2 \times 1.29 \times 10^{-11} \text{ GeV}$$

(two-body kinematics, no contact term),

$$\Gamma = |V_{ub}|^2 \times 1.41 \times 10^{-11} \text{ GeV}$$

(narrow-width approximation, no contact terms),

$$\Gamma = |V_{ub}|^2 \times 62.0 \times 10^{-11} \text{ GeV} \quad (60)$$

(two-body kinematics with contact terms),

and, for $I=0.33$ and a dipole form factor,

$$\Gamma = |V_{ub}|^2 \times 1.01 \times 10^{-11} \text{ GeV}$$

(two-body kinematics, no contact terms),

$$\Gamma = |V_{ub}|^2 \times 1.09 \times 10^{-11} \text{ GeV}$$

(narrow-width approximation, no contact terms),

$$\Gamma = |V_{ub}|^2 \times 103 \times 10^{-11} \text{ GeV} \quad (61)$$

(two-body kinematics with contact terms).

These results can also be expressed as branching ratios using the lifetime quoted above:

$$B(B^- \to \rho^0 e^- \nu) = 1112 |V_{ub}|^2 ,$$

(two-body kinematics with contact terms)

for a monopole form factor and $I=0.33$,

$$B(B^- \to \rho^0 e^- \nu) = 1859 |V_{ub}|^2 ,$$

(two-body kinematics with contact terms)

for a dipole form factor and $I=0.33$. Comparing to the recent CLEO result,[20] Eq. (58), we find the limits

$$|V_{ub}| < 5.19 \times 10^{-4}$$

(two-body kinematics with contact terms)

for a monopole form factor and $I=0.33$,

$$|V_{ub}| < 4.02 \times 10^{-4}$$

(two-body kinematics with contact terms)

for a dipole form factor and $I=0.33$.

Striking here is the dramatic effect of the contact terms, which boost the rate by two orders of magnitude. Further analysis reveals the effect to be primarily the vector contact term; putting it to zero results only in a doubling of the rate. The presence of the contact terms has been suggested by the extrapolation of a current-algebra result to very high energy, admittedly a crude estimate, but in the absence of a detailed dynamical theory for these current-algebra "backgrounds," they cannot be ruled out. The moral seems to be that extraction of V_{bu} from these rates through their contributions to the electron end-point spectrum seems to be a very difficult task that will require careful study of high-statistics data such as those which might be available from a B factory to see whether or not such nonresonant background is present.

IV. SUMMARY AND CONCLUSIONS

In this work we have incorporated the "low-energy" results of chiral symmetry into resonance decay models for semileptonic decays of D and B mesons to two pseudoscalar mesons. The resonance models for $D \to K^*$, $D \to \rho$, $B \to D^*$, and $B \to \rho$ were considered in the zero-width approximation and with finite-width effects with and without the contact terms originating from the low-energy effective Lagrangian. The weak transition matrix elements between D and B mesons and the intermediate vector mesons have sufficient structure so that there are no unjustified constraints on the three independent helicity structure functions H_+, H_-, and H_0 as was the case in many of the older works. The dependence of the lepton spectrum on the form factors F^V and F_2^A and the variation of the asymmetry parameter α as a function of F_2^A/F_1^A were studied in detail. The results for α were compared to experimental data in the cases $D \to K^*$ and $B \to D^*$.

The finite-width effect for $D \to K^* \to K\pi$ is approximately 11%. The background described by contact terms increases the width by 7%, in reasonable agreement with the data from the E691 experiment at Fermilab. For $D \to \rho \to \pi\pi$ the finite-width effect and the background contributions are much larger. Taking the same overlap factor I as for $D \to K^*$, the finite-width effect causes the partial semileptonic width to decrease by 16% and the contact terms increase the width by 9%. This is clearly connected to the larger width of the ρ as com-

pared to the K^* width. Clearly there are no such effects for $B \to D^* \to D\pi$ because of the extremely small total width of the D^*. On the other hand, for $B \to \rho \to \pi\pi$ these effects are large again. The finite-width effect is only 9%, but the contribution of the contact terms is huge. This is partly due to the assumed small overlap factor in the resonance transition and partly due the large energy difference between initial and final states. Although we expect that these large background terms as described by the low-energy contact terms will be modified by higher-derivative terms and higher-order loop corrections, our result indicates that the $B \to \rho \to \pi\pi$ transition is much less suitable for determining V_{ub} from experimental data to be obtained in the future. To get information on V_{ub} the single-pion final state seems much more suitable although it also depends on one unknown form factor which, however, is under much better theoretical control than the background terms in the $\pi\pi$ final state.

Accurate experimental data on the partial semileptonic widths, the lepton spectrum and the asymmetry parameter α are needed to determine the universal overlap factor I and the relative magnitude of the vector-meson form factors F_V, F_1^A, and F_2^A. The parameter α has been measured for $D \to K^*$ and $B \to D^*$, although with large errors. From these data it seems that the ratio F_2^A/F_1^A for both decays is not in agreement with $-2/(m_p + m_v)^2$ advocated in the work of Körner and Schuler.[8]

Note added in proof. After submission of this paper it was brought to our attention that the CLEO results[20] in Eqs. (54) and (58) are based on electron energies between 2.3 and 2.7 GeV. If we include in our branching ratios only electron energies above 2.3 GeV the results of Eq. (53) are reduced by factors 7.19 (for the monopole form factor) and 2.52 (for the dipole form factor), respectively. Similarly the branching ratios in Eq. (57) are reduced by factors 4.04 and 3.18. This increases the upper limits in Eq. (55) to 4.77×10^{-3} (monopole form factor) and to 1.44×10^{-3} (dipole form factor) and those in Eq. (59) to 2.29×10^{-3} (monopole form factor) and to 2.30×10^{-3} (dipole form factor), respectively. The limits following from two-body kinematics with contact terms are 3.11×10^{-3} and 1.92×10^{-3} instead of 5.19×10^{-4} and 4.02×10^{-4}.

ACKNOWLEDGMENTS

This work was supported in part by the U.S. Department of Energy. One of the authors (W.F.P.) wishes gratefully to acknowledge the hospitality of the II. Institut für Theoretische Physik der Universität Hamburg and the partial support of the Deutscher Academischer Austausch Dienst.

[1] M. K. Gaillard, B. W. Lee, and T. L. Rosner, Rev. Mod. Phys. **47**, 277 (1975); J. Ellis, M. K. Gaillard, and D. V. Nanopoulos, Nucl. Phys. **B100**, 313 (1975); A. Ali, Z. Phys. C **1**, 1 (1979).

[2] A. Ali and E. Pietarinen, Nucl. Phys. **B154**, 519 (1979); N. Cabibbo, G. Corbo, and L. Maiani, *ibid.* **B155**, 93 (1979); G. Altarelli, M. Cabibbo, G. Corbo, and L. Maiani, *ibid.* **B208**, 365 (1982).

[3] N. Isgur, D. Scora, B. Grinstein, and M. B. Wise, Phys. Rev. D **39**, 799 (1989).

[4] For most recent reviews, see D. Hitlin, in *Lepton and Photon Interactions,* proceedings of the International Symposium on Lepton and Photon Interactions at High Energies, Hamburg, West Germany, 1987, edited by W. Bartel and R. Rückl [Nucl. Phys. B, Proc. Suppl. **3** (1988)]; D. M. Coffman, Report No. CALT-68-1415, 1987 (unpublished); H. Schröder, DESY Report No. 88-101, 1988 (unpublished).

[5] J. C. Anjos *et al.*, Phys. Rev. Lett. **62**, 722 (1989); **62**, 1587 (1989).

[6] H. Albrecht *et al.*, Phys. Lett. B **197**, 452 (1987).

[7] A. Ali and T. C. Yang, Phys. Lett. **65B**, 275 (1976).

[8] I. Hinchliffe and C. H. Llewellyn Smith, Nucl. Phys. **B114**, 45 (1976); G. L. Kane, Phys. Lett. **70B**, 227 (1977); W. J. Wilson, Phys. Rev. **16**, 742 (1977); V. Barger, T. Gottschalk, and R. J. N. Phillips, *ibid.* **16**, 746 (1977); F. Bletzacker, M. T. Nieh, and A. Soni, *ibid.* D **16**, 732 (1977); X. Y. Pham and J. M. Richard, Nucl. Phys. **B128**, 453 (1978); D. Fakirov and B. Stech, *ibid.* **B133**, 315 (1978); M. B. Gavela, Phys. Lett. **83B**, 367 (1979); A. Ali, J. G. Körner, G. Kramer, and J. Willrodt, Z. Phys. C **1**, 269 (1979); M. Suzuki, Phys. Lett. **155B**, 155 (1985); Nucl. Phys. **B258**, 553 (1985); M. Wirbel, B. Stech, and M. Bauer, Z. Phys. C **29**, 637 (1985); B. Grinstein, M. B. Wise, and N. Isgur, Phys. Rev. Lett. **56**, 298 (1986); F. Schöberl and H. Pietschmann, Europhys. Lett. **2**, 583 (1986); T. Altomari and L. Wolfenstein, Phys. Rev. Lett. **58**, 1563 (1987); S. Nussinov and W. Wetzel, Phys. Rev. D **36**, 130 (1987); J. G. Körner and G. A. Schuler, Z. Phys. C **38**, 511 (1988); M. Bauer and M. Wirbel, *ibid.* **42**, 671 (1989).

[9] S.-C. Chao, G. Kramer, W. F. Palmer, and S. Pinsky, Phys Rev. D **30**, 1916 (1984); S.C. Chao, R. Kass, G. Kramer, W. F. Palmer, and S. Pinsky, *ibid.* **31**, 1756 (1985).

[10] G. Kramer and W. F. Palmer, Phys. Rev. D **36**, 154 (1987). See also G. Kramer and W. F. Palmer, Z. Phys. C **39**, 423 (1988).

[11] Pham and Richard (Ref. 8); Körner and Schuler (Ref. 8).

[12] Wirbel, Stech, and Bauer (Ref. 8).

[13] C. A. Dominguez and N. Paver, Phys. Lett. B **207**, 499 (1988); Z. Phys. C **41**, 217 (1988).

[14] Ali, Körner, Kramer, and Willrodt (Ref. 8).

[15] R. Morrison, DESY Report No. T-88-01, 1988 (unpublished).

[16] If future experiments should confirm the Mark III results, they could perhaps be accommodated within the present framework by including effects of higher-derivative contact terms, some of which have been determined from π-π scattering by J. F. Donoghue, C. Ramirez, and G. Valencia, Phys. Rev. D **38**, 2195 (1988).

[17] E. Braaten, R. J. Oakes, and Sze-Man Tse, Phys. Rev. D **36**, 2188 (1987).

[18] C. A. Dominguez, Mod. Phys. Lett. A **2**, 983 (1987).

[19] H. Albrecht *et al.*, Phys. Lett. B **219**, 121 (1989).

[20] Sheldon Stone, in *Proceedings of the XIX International Symposium on Multiparticle Dynamics,* Arles, France, 1988 (CLNS Report No. 88/855, Cornell University, Ithaca, NY, 1988).